ACTA METALLURGICA SLOVACA
2022, VOL. 28, NO. 2, 101-105

RESEARCH PAPER

CONTROL OF THE PROCESSES OF PHASE FORMATION OF CARBIDE COMPONENTS IN NICKEL-BASED SUPERALLOYS

Alexander Anatolyevich Glotka[1], Vadim Efimovich Ol'shanetskii[1]*

[1] *Zaporizhzhia Polytechnic National University, Ukraine, Zaporizhzhia, st.Zhukovskogo, 64, 69063*

*Corresponding author: glotka-alexander@ukr.net, tel.: +380964275651, Zaporizhzhia Polytechnic National University, Ukrai-ne, Zaporizhzhia, st. Zhukovskogo, 64, 69063

Received: 23.05.2022
Accepted: 25.05.2022

ABSTRACT

The mathematical dependences of thermodynamic processes of precipitation of carbide phases are determined, and a practical study of the structure and distribution of chemical elements is carried out. Regularities were established for the effect of the chemical composition of the alloy on the morphology and type of carbides. It is shown that, depending on the introduced chemical elements in the system, the types of carbides and their chemical composition can change, which leads to a decrease in the processes of crack formation in the material. The established dependencies for the multicomponent system Ni-22.5Cr-19Co-1.9Al-3.7Ti-2W-1.4Ta-1Nb-0.15C make it possible to determine the chemical composition of carbides from the chemical composition of the alloy. The evaluation of the results obtained by the calculation method and experimental data was carried out, and the analysis of the results gave good convergence and can be recommended for industrial use.

Keywords: phase formation, weldable nickel-based superalloy, carbides, distribution of alloying elements, precipitation (dissolution) temperatures of carbides

INTRODUCTION

Carbides of the MC type are formed during crystallization in the form of discrete particles in the intergranular and intragranular space, as well as in the interdendritic regions in the liquid due to the strong segregation of carbon when its amount is above 0.05%, and also at temperatures slightly below the solidification temperature of the alloy. In carbide reactions in alloys, they are the main source of carbon. In order of decreasing stability in heat-resistant nickel alloys, carbides are placed in the series HfC, TaC, NbC, TiC [1-9]. These carbides are very stable at low temperatures, but at higher temperatures, they tend to convert (degrade) into secondary carbides of various types.

The impact of carbides is complex, located along the boundaries or inside the grains, they perform a modifying function, helping to prevent recrystallization, atoms of various elements can replace each other in the carbide, thereby changing the morphology of precipitates.

The shape of carbides has a significant effect on the plasticity of cast nickel superalloys; in the case of the formation of "Chinese hieroglyphs," it is much lower than in the case of the formation of a spherical precipitate. The size of carbides can also affect the heat resistance [10-12]. Sufficiently large carbides at the grain boundaries reduce the creep and fatigue resistance of the alloys due to the high difference between the elastic moduli of the carbides and the matrix. Also, carbides can be destroyed during thermal cycling (starting and stopping the engine) due to cracking [13-24].

The purpose of the work is to optimize the chemical composition and morphology of carbides of welded nickel-based superalloys by changing the chemical composition of the alloy, which will increase the performance properties of body parts.

MATERIAL AND METHODS

Modelling the processes of precipitation of carbides using the CALPHAD method makes it possible to carry out the computational prediction and a comparative assessment of the influence of alloying elements in carbides. Calculations were carried out for each studied composition individually with a step-by-step change of a specific alloying element into a fixed composition of a multi-component system.

In the system (Ni-22.5Cr-19Co-1.9Al-3.7Ti-2W-1.4Ta-1Nb-0.15C), the range of element variation was chosen based on considerations of the maximum and minimum amount of the element introduced into the nickel-based superalloys. Thus, carbide-forming elements were chosen for the study in the following alloying ranges: carbon 0.02-0.2%; niobium 0.1-4%; titanium 1-6%; tantalum 0.5-12%, tungsten 1-16%, chromium 1-35% by weight.

The alloy crystallization process was modelled by the CALPHAD method from the liquid state temperature (1600°C) to room temperature (20°C) with a temperature step of 10°C over the entire range, which made it possible to determine the temperature sequence of phase separation during crystallization. Calculations were carried out on the initial chemical composition of the alloy with the determination of the most probable precipitation of the amount and type of carbides in the structure, as well as their chemical composition after modelling the crystallization process.

The composition of carbides was experimentally determined on a REM-106I scanning electron microscope with an energy-dispersive X-ray spectral microanalysis system. This method was used to study morphology and chemical composition of precipitated carbides in the alloy structure. The conversion of qualitative values into quantitative analysis was carried out automatically according to the device program. The relative

error of the method is ± 0.1% (by mass). The results of calculations of the type of carbides and their chemical composition were compared with experimental data obtained using electron microscopy.

RESULTS AND DISCUSSION

Modern gas turbine engines require materials with improved performance, extended overhaul intervals and high heat resistance and maintainability. These are the requirements that are imposed when designing new materials for body parts of unmanned aerial vehicles and gas turbine units of gas-pumping equipment. The properties of high-temperature materials are ensured by the stability of the structural components during operation. A very important parameter for heat treatment is the carbide liquidus temperature, which also affects the operating temperatures of the parts. It has been established that with an increase in the carbon content in the alloy, an increase in the carbide liquidus temperature t_L and the number of carbides in the composition of the alloy is observed (**Fig. 1**). This leads to a deterioration in the operational and repair properties of the material due to the formation of coarse inclusions of carbide components. The above feature should be taken into account and rational doping limits should be chosen, which lie in the range of 0.1-0.15% carbon.

The temperature of the carbide liquidus decreases with an increase in the titanium content in the alloy (**Fig. 2, a**), this is due to precipitation by a change in the composition of the carbide (**Fig. 2 b**). So, at a titanium concentration in the alloy of more than 3%, its amount begins to prevail in the carbide over the amount of niobium, and at a concentration of more than 5.5% over the amount of tantalum. The transformation of the composition of carbides obeys linear laws and is described by the corresponding mathematical dependencies, which are presented in **Table 1**. Changes in the composition of carbides lead to a change in their morphology. Carbides of the TiC type precipitate in interdendritic spaces and have a font ("Chinese hieroglyphs") shape, which negatively affects the properties of the alloy, so it is necessary to limit alloying and prevent their precipitation. In the test composition, the titanium content should not exceed 5.5%.

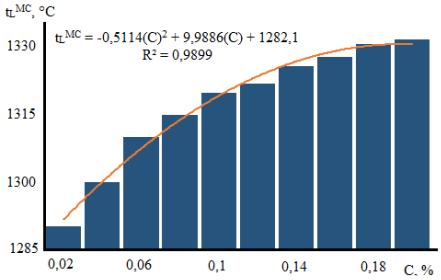

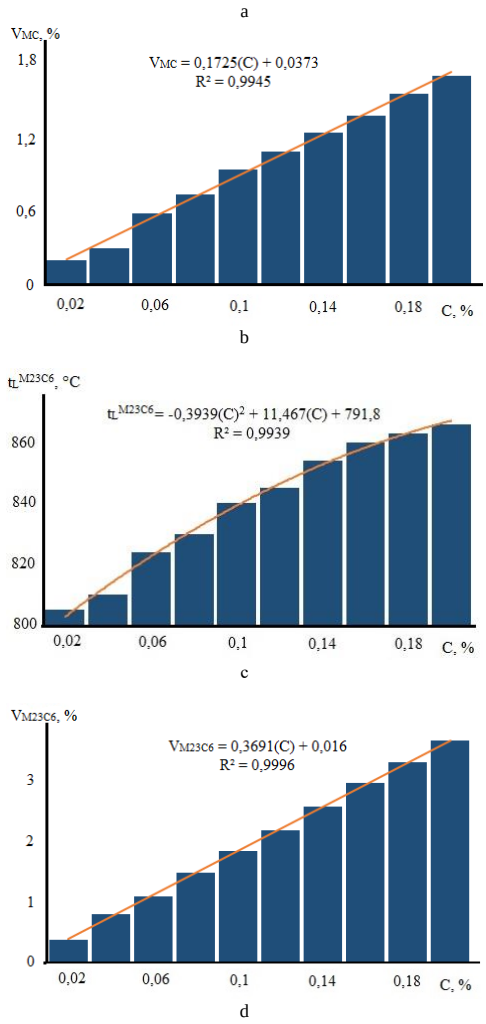

Fig. 1. - Temperature dependences of the dissolution (precipitation) of MC (a) and $M_{23}C_6$ (b) type carbides, as well as the amount of MC (c) and $M_{23}C_6$ (d) carbides on the carbon content in the alloy.

Table 1 - Dependences of the content of alloying elements in carbides on the content of alloying elements in the alloy.

Alloying element	Dependences of the content of elements in carbide, % mass
Ta	C_{Ta} = -0,7425(C_{Ta} in alloy)² + 13,919(C_{Ta} in alloy) + 13,708, R² = 0,9541; C_{Ti} = 0,388(C_{Ta} in alloy)² - 7,0591(C_{Ta} in alloy) + 39,156, R² = 0,9638; C_{Nb} = 0,2588(C_{Ta} in alloy)² - 4,7618(C_{Ta} in alloy) + 28,039, R² = 0,9552.
Ti	C_{Ta} = -1,28(C_{Ti} in alloy) + 42,898, R² = 0,899; C_{Ti} = 4,4782(C_{Ti} in alloy) + 10,454, R² = 0,9789; C_{Nb} = -3,95(C_{Ti} in alloy) + 36,12, R² = 0,988.
Nb	C_{Nb} = 13,038(C_{Nb} in alloy) + 6,0995, R² = 0,9728; C_{Ta} = -5,253(C_{Nb} in alloy) + 43,374, R² = 0,9866; C_{Ti} = -6,8196(C_{Nb} in alloy) + 35,929, R² = 0,9619.
W	C_{Cr} = 0,1236(C_W in alloy)² - 2,7352(C_W in alloy) + 84,886, R² = 0,9138 C_W = -0,1478 (C_W in alloy)² + 3,3042 (C_W in alloy) + 2,8098, R² = 0,9374

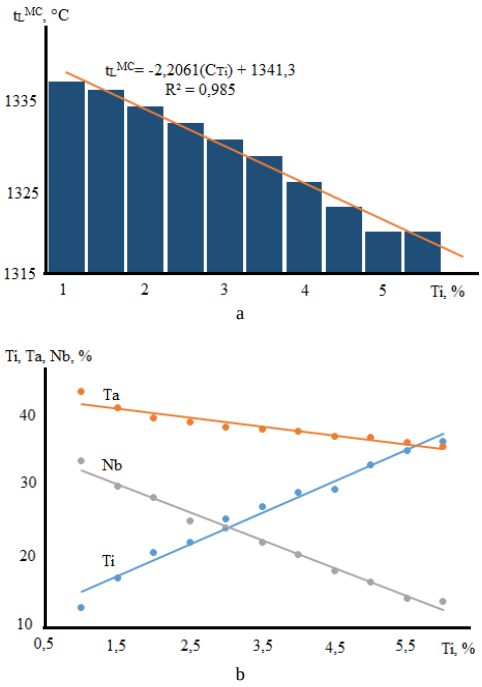

Fig. 2. - Temperature dependence of the dissolution of MC type carbides (a) and the amount of tantalum, titanium and tungsten in MC carbide (b) on the titanium content in the alloy

An increase in the carbide liquidus temperature t_L with an increase in the amount of tantalum in the alloy is associated with the formation of TaC carbides already at a concentration of more than 1% tantalum in the alloy (**Fig. 3**). The transition of MC carbide to tantalum-based carbide leads to an increase in interatomic bonds, which contributes to an increase in the dissolution (precipitation) temperature of the carbide. However, at 2% tantalum, a topologically close-packed η-phase (61.3Ni-15.4Co-13.7Ti-4.8Nb-2.34Ta-2.08Al-0.29Cr) appears in the composition, which must be taken into account when modernizing the alloy. Also, at 7% tantalum in the alloy, carbides of the $M_{23}C_6$ type degenerate and this negatively affects the grain boundary creep at operating temperatures. The introduction of tantalum changes the MC carbide morphology to a faceted irregular shape.

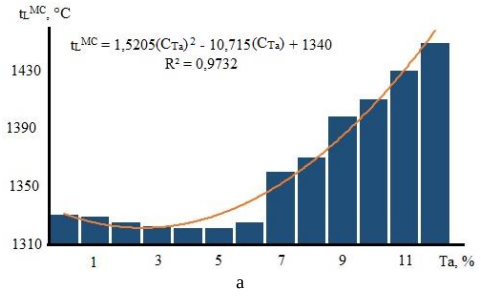

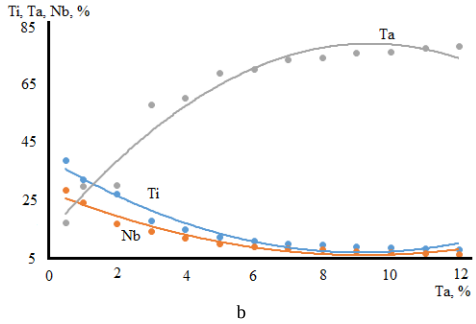

Fig. 3. - Temperature dependence of the dissolution of MC type carbides (a) and the amount of tantalum, titanium and niobium in MC carbide (b) on the tantalum content in the alloy

The introduction of niobium into a complexly alloyed composition leads to a decrease in the temperature of the carbide liquidus at a concentration of 2.5–3% (**Fig. 4**). In the same doping range, the appearance of the η-phase is observed, after the formation of which there is an increase in t_L, as well as a change in the base of the carbide to NbC. Niobium carbide does not have a high liquidus temperature, it is not much lower than TaC carbide and significantly lower than TiC, thus, one should strive not for the formation of monocarbides based on a single element, but for the formation of complex carbides based on more than one element.

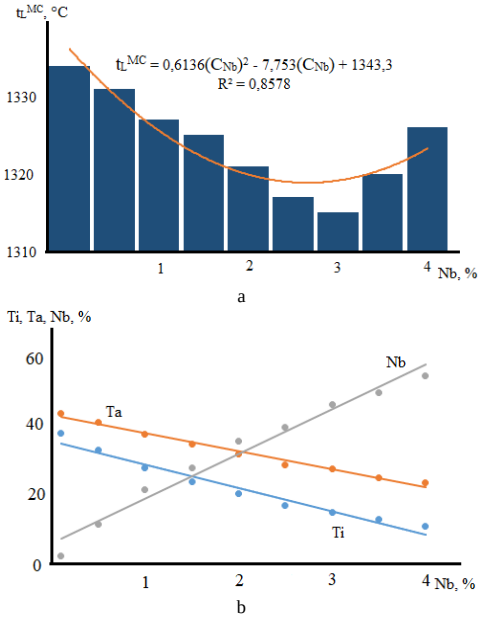

Fig. 4. - Temperature dependence of the dissolution of MC type carbides (a) and the amount of tantalum, titanium and niobium in MC carbide (b) on the niobium content in the alloy

Chromium is an element that influences the formation of secondary carbides, it has a significant effect on the temperature of dissolution (precipitation) of carbides. It has been established that carbides of the $M_{23}C_6$ type begin to precipitate

from the solid solution at a concentration of 17% chromium (**Fig. 5**), which is described by a parabolic dependence. The composition of carbides practically does not change with an increase in chromium in the alloy and is at the level of 80.5Cr-8.5W-4Co-2Ni. However, at 31% Cr, a BCC (chromium-based solid solution) phase is formed in the alloy, which significantly reduces the mechanical properties.

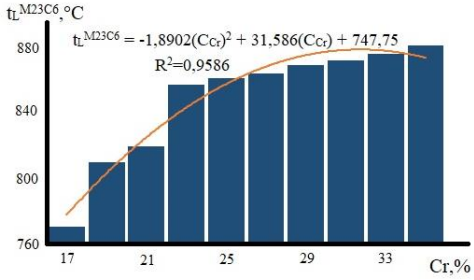

Fig. 5. - Temperature dependence of the dissolution (precipitation) of $M_{23}C_6$ type carbides on the chromium content in the alloy composition

An increase in tungsten in the composition of the alloy leads to a decrease in the temperature of the carbide liquidus at a concentration of more than 6% (**Fig. 6**), this behaviour is associated with the formation of a σ-phase, the crystal lattice of which is close to $M_{23}C_6$, with a ratio of dimensional parameters $c/0{,}52 \approx a$ and chromium concentration 52%. The appearance of this phase affects the thermodynamics of processes in the alloy and reduces the heat resistance of the material. Also, with an exaggeration of more than 8% W, a μ-phase is formed in the alloy, the crystal lattice of which approaches M_6C, according to a similar mechanism to the σ-phase, which also reduces the mechanical properties.

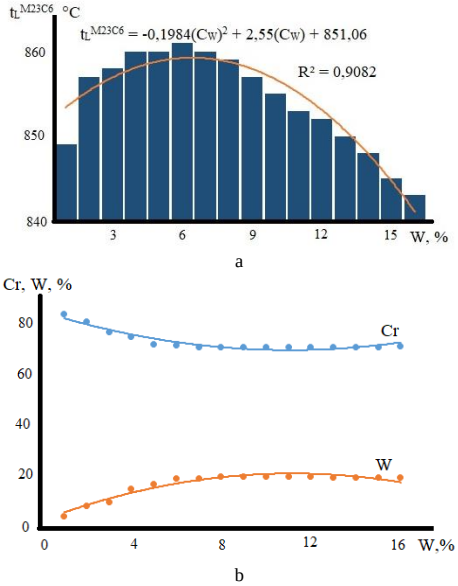

Fig. 6. - Temperature dependence of the dissolution of $M_{23}C_6$ type carbides (a) and the amount of chromium and tungsten in $M_{23}C_6$ carbide (b) on the tungsten content in the alloy

The established dependences of the effect of the chemical composition of the alloy on the composition of carbides of the nickel-based superalloy of the Ni-22.5Cr-19Co-1.9Al-3.7Ti-2W-1.4Ta-1Nb-0.15C system were checked on a REM-106I scanning electron microscope with X-ray spectral microanalyzer system. The morphology of MC carbides has the form of both individual blocks and «Chinese hieroglyphs» (**Fig. 7**). Carbides of the $M_{23}C_6$ type are present in the form of discontinuous block and lamellar forms (**Fig. 7**) that stand out along the grain boundaries. The most rational and thermodynamically advantageous is the block type of carbide precipitates since in this case the stress concentration with the matrix is at the lowest possible level.

The structures presented in **Fig. 7** are a consequence of the redistribution of elements in the alloy matrix and carbide phases. The structural-energy state, which determines the morphology of carbides, is associated with a change in the composition of the carbide phases (in the process of dissolution-precipitation) and a change in the relative free energies of the boundaries.

The chemical composition of the carbides was determined experimentally by X-ray spectral microanalysis, with which the intensity of X-ray radiation was recorded depending on the energy keV. It has been experimentally established that titanium, niobium, tungsten, molybdenum, nickel, and chromium are included in the composition of carbides in the following ratios in comparison with the calculated values (**Table 2**).

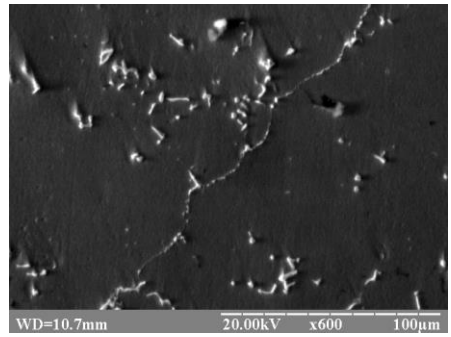

a

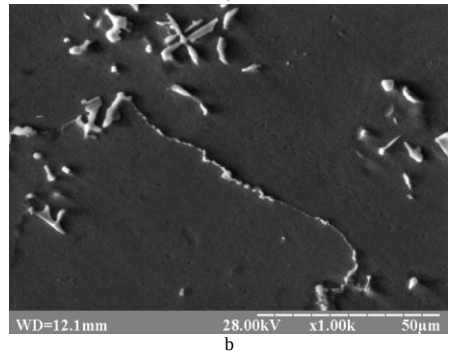

b

Fig. 7. - Morphology of carbides in the alloy structure of the Ni-22,5Cr-19Co-1,9Al-3,7Ti-2W-1,4Ta-1Nb-0,15C system

Table 2 shows that the calculated and experimental data are in good agreement with each other for almost all elements. There is an increased content of tantalum and niobium in primary carbides and chromium in secondary carbides. It is experimentally confirmed that the data obtained by calculation (according

to the established regression models) and experimental methods have an error not exceeding 3%.

Thus, the calculated data for determining the type and chemical composition of carbides showed good convergence and agreement with experimental data obtained by electron microscopy.

Table 2 Chemical composition of carbides calculated from certain dependencies and obtained experimentally by X-ray spectral microanalysis at 20°C

Method of obtaining results	Element content, % wt.							
	Ti	Nb	W	Ta	Ni	Cr	Co	C
Estimated composition MC	27,9	21,7	0,9	37,7	-	0,19	-	11,4
Estimated composition $M_{23}C_6$	-	-	9,14	-	1,7	80,5	3,38	5,3
Composition of the carbide type has been experimentally established MC (**Fig. 7**)	25,6	22,5	0,5	39,6		0,32		11,4
The composition of the carbide type has been experimentally established $M_{23}C_6$ (**Fig.7**)	-	-	6,8	-	1,1	83,2	2,6	5,3

CONCLUSIONS

1. Based on modern ideas about the concept of phase formation in high-temperature nickel alloys, carbides are an integral part of the system that affect the properties and require composition adjustment. Regularities have been established for the effect of the chemical composition of the alloy on the morphology and type of carbides. It is shown that, depending on the introduced chemical elements in the system, the types of carbides and their chemical composition can change, which leads to a decrease in the processes of crack formation in the material.
2. Mathematical dependencies have been established, by which it is possible to determine the liquidus temperature of carbides, which makes it possible to optimize the heat treatment modes to obtain the optimal structure of the alloys.
3. It has been established that with an increase in the titanium concentration of more than 5.5%, a η-phase is formed, and MC-type carbides acquire a font shape, which reduces the fracture toughness of the material. Also, the η-phase is formed at a concentration of more than 2% Ta in the alloy, and already at 7%, degeneration of carbides of the $M_{23}C_6$ type occurs, which negatively affects the grain boundary creep. The introduction of more than 2.5% Nb leads to the formation of a topologically close-packed phase and a decrease in the heat resistance characteristics of the material.
4. A comparative evaluation of the calculated results obtained by regression models and experimental data obtained by X-ray spectroscopy was carried out. Analysis of the results gave good convergence and can be proposed for predicting structural components both in industrial alloys and in the development of new materials.

REFERENCES

1. A. Mitchell, S. L. Cockcroft, C. E. Schvezov: High Temperature Materials Processes, 15, 1996, 27-40. https://doi.org/10.1515/HTMP.1996.15.1-2.27.
2. A. Sadeghian, S.E. Mirsalehi, F. Arhami: Metallurgical and Materials Transactions A, 52, 2021, 1526–1539. https://doi.org/10.1007/s11661-021-06176-x.
3. A. Orozco-Caballero, C. Gutierrez, B. Gan: Journal of Materials Research, 36, 2021, 2213–2222. https://doi.org/10.1557/s43578-021-00133-5.
4. N. Lv D. Liu, Y. Yang: The International Journal of Advanced Manufacturing Technology, 112, 2021, 3415–3429. https://doi.org/10.1007/s00170-021-06612-7.
5. A. Ota, N. Ueshima, K. Oikawa, S. Imano: Microstructure Controlling of U720-Typed Superalloys to Improve a Hot and Cold Workability by Using Incoherent Gamma Prime. *Proceedings of the 9th International Symposium on Superalloy 718 & Derivatives: Energy, Aerospace, and Industrial Applications*. The Minerals, Metals & Materials Series. Springer, Cham. https://doi.org/10.1007/978-3-319-89480-5_66.
6. M. Sedighi, Y. Shajari, S.H. Razavi: Protection of Metals and Physical Chemistry of Surfaces, 57, 2021, 113–120. https://doi.org/10.1134/S2070205120060210.
7. D. Liu, X. Cheng, X. Zhang: Journal of Wuhan University of Technology-Mater. Sci. Ed., 31, 2016, 1368–1376. https://doi.org/10.1007/s11595-016-1540-3.
8. O.A. Glotka: Journal of Achievements in Materials and Manufacturing Engineering, 102, 2020, 5-15. https://doi.org/10.5604/01.3001.0014.6324.
9. J. Dutkiewicz, W. Maziarz: Acta Metallurgica Slovaca, 20, 2017, 265-270. https://doi.org/10.12776/ams.v20i3.305.
10. E., Cortes, A., Bedolla-Jacuinde, M,. Rainforth:. Journal of Materials Engineering and Performance, 28, 2019, 4171–4186. https://doi.org/10.1007/s11665-019-04179-9.
11. S.Yu. Kondrat'ev, E.V. Sviatysheva, G.P. Anastasiadi, S.N. Petrov: Acta Materialia, 127, 2017, 267-276. https://doi.org/10.1016/j.actamat.2017.01.043.
12. S. Lissarrague, M.H. Buitrago, A.S. Picasso: Acta Metallurgica Slovaca, 25(3), 2019, 180-185. https://doi.org/10.12776/ams.v25i3.1312.
13. P. Jonšta, Z. Jonšta, J. Sojka: Journal of Achievements in Materials and Manufacturing Engineering 21, 2017, 29-32.
14. L. Jiang, W. Z. Zhang, Z. Feng: Materials & Design, 112, 2016, 300-308. https://doi.org/10.1016/j.matdes.2016.09.075.
15. H. Rui , L. Jinshan, B. Guanghai: Materials Science and Engineering A, 548, 2012, 83-88. https://doi.org/10.1016/j.msea.2012.03.092.
16. Y. Chen, H.M. Wang: Journal of Materials Research, 21, 2006, 375–379. https://doi.org/10.1557/jmr.2006.0043.
17. Y.H. Kong, Q.Z, Chen, D.M. Knowles: Journal of Materials Science, 39, 2004, 6993–7001. https://doi.org/10.1023/B:JMSC.0000047543.64750.83.
18. S. Tin, T.M. Pollock, W. Murphy: Metallurgical and Materials Transactions A, 32, 2001, 1743–1753. https://doi.org/10.1007/s11661-001-0151-5.
19. N.V. Petrushin, E.M. Visik, M.A. Gorbovets: Russian Metallurgy (Metally), 45, 2016, 630–641. https://doi.org/10.1134/S0036029516070119.
20. A.A. Glotka: Acta Metallurgica Slovaca, 27, 2021, 68-71. https://doi.org/10.36547/ams.27.2.813.
21. Z. Yu, J. Qiang, J. Zhang: Journal of Materials Research, 30, 2015, 2064–2072. https://doi.org/10.1557/jmr.2015.127.
22. G.D. Pigrova, A.I. Rybnikov: The Physics of Metals and Metallography, 114, 2013, 593–595. https://doi.org/10.1134/S0031918X13070089.
23. V. Efremenko, R. Kussa, I. Petryshynets, K. Shimizu, Kromka, F. Zurnadzhy, V. Gavrilova: Acta Metallurgica Slovaca, 26(3), 2020, 116-121. https://doi.org/10.36547/ams.26.3.554.
24. A. A. Glotka, A. N. Moroz: Metal Science and Heat Treatment, 61, 2019, 521-524. https://doi.org/10.1007/s11041-019-00456-5.